Accepted Manuscript

An o-hydroxyl aldehyde structure based naphthalimide derivative: Reversible photochromic properties and its application in ClO− detection in living cells

Xinxue Tang, Hao Sun, Jing Nie, Xiang'en Han, Yun Zhao, Ran Zhang, Zhonghai Ni

PII:	S1386-1425(19)30430-5
DOI:	https://doi.org/10.1016/j.saa.2019.04.049
Reference:	SAA 17057
To appear in:	*Spectrochimica Acta Part A: Molecular and Biomolecular Spectroscopy*
Received date:	27 February 2019
Revised date:	12 April 2019
Accepted date:	18 April 2019

Please cite this article as: X. Tang, H. Sun, J. Nie, et al., An o-hydroxyl aldehyde structure based naphthalimide derivative: Reversible photochromic properties and its application in ClO− detection in living cells, Spectrochimica Acta Part A: Molecular and Biomolecular Spectroscopy, https://doi.org/10.1016/j.saa.2019.04.049

An o-Hydroxyl Aldehyde Structure Based Naphthalimide Derivative: Reversible Photochromic Properties and Its Application in ClO^- Detection in Living Cells

Xinxue Tang, Hao Sun, Jing Nie, Xiang'en Han*, Yun Zhao, Ran Zhang, Zhonghai Ni*

School of Chemical Engineering and Technology, China University of Mining and Technology, Xuzhou221116, People's Republic of China;

Corresponding author E-mail: xiangenh@163.com (X. E. Han) and nizhonghai@cumt.edu.cn (Z. H. Ni)

Abstract:

A bifunctional organic compound 2-butyl-6-hydroxy-1,3-dioxo-2,3-dihydro-1H-benzo[de] isoquinoline-5-carbaldehyde (**BHC**) with photochromic properties in solid state and probe detection for ClO^- in complete water solution was synthesized and fully characterized. A 'white–yellow–white' reversible photochromic behavior could be observed when alternating UV/vis light irradiation on the solid **BHC** powder. Good fatigue resistance and adjustable bleaching rate were shown when heating conditions changes. In addition, **BHC** displayed a high selectivity and low detection limit (1.16×10^{-8} M) for ClO^-. The photoluminescent fluorescence "on-off" recognition result can be easily identified and **BHC** has been tested for safely imaging living cells and detecting hypochlorite anion in vitro and vivo. A better water solubility of **BHC** effectively reduces damage caused by organic solvent in cell imaging progress.

Keywords: Reversible photochromic; Fatigue resistance; ClO^- detection; Cell imaging; Water solubility;

1 Introduction

Organic photoactive materials, which could switch their optical signals towards the external stimulation or output the bright multi-colors in different environments [1], have attracted much attention for the potential applications in fluorescent sensors, organic light emitting diodes (OLED) [2, 3] and biological imaging in the past few decades [4-6]. Among many research fields, exploiting the inherent diversity of compounds to take full advantages of molecular properties and maximize the use of materials has been paid much attention by many researchers [7, 8]. Naphthalimide, as a

typical chromophore, has been extensively designed and widely used as molecular sensor [9] and cell imaging material [10], which is based on its unique fluorescent properties such as strong fluorescence, high sensitivity, good light stability and be stable in the physiological pH range [11]. At the same time, the emission signal of such an attractive fluorophore can be detected easily, which dramatically expand the range of practically useful applications of fluorescent part and make them potentially used for optical signal storage and collection, like photochromic compounds had done [12-14]. These compounds are powerful research objects for bifunctional and multifunctional material [15].

Since Hirshberg had proposed concept of photochromism, photochromic compounds have been the focus of high-density information storage and recording functional materials [16, 17]. The use of photochromic compounds, such as Schiff bases, diarylethene and spiropyran, as photo switching systems attracts much attention because of their potential ability for application in photonic devices [18]. Among various photochromic compounds, Schiff base is one of the most important class of these materials [19-21]. They have good chemical stability and anti-degradation ability under illumination, like salicylaldehyde based Schiff base. These compounds may undergo photochromic behavior in solid state and crystalline state, which expands the application in optical devices and anti-counterfeiting fields [22]. Their discoloration is a light-induced proton transfer process. Specifically, it is a proton easy to escape and a pairs of electrons provided by nitrogen atoms in adjacent positions will attract it. In the excited state, it is relatively prone for proton to transfer from the oxygen atom in Phenolic hydroxyl to the nitrogen atom, resulting in a color change. In addition to the nitrogen atom, the oxygen atom and sulfur atom have a similar electron donating structure [23, 24]. However, such phenomena is rarely found in an ortho-hydroxy aldehyde compound who shares the same potential proton transfer ability. In 2017, Chen and his coworkers had designed and synthesized several naphthaldehyde molecules and tried to find out the excited state intramolecular proton transfer (ESIPT) between aldehyde and hydroxyl group, moving multiple protons across a bridging hydrogen bond (H-bond) [25]. Nevertheless, this research was conducted in the polar, aprotic solvents, which make a big difference compared with the solid state.

Research on the development of photochromic compounds in solid and crystalline states remains attractive, and this expansion of photochromic compounds based on the ESIPT mechanism will be a

promising result in more sensors and smart materials application area [26].

In addition to applications of optical devices, many researchers have also focused on bio-probes these are able to detect various substances, ions and reactive oxygen species (ROS) in cells in order to efficiently utilize various excellent properties of organic photo luminescent compounds [27-32].

Hypochlorite (ClO^-), a daily used disinfectant, is an essential member of reactive oxygen species (ROS) in living organism and plays a vital role in the immune system due to its antibacterial properties [33-35]. Organisms produce ROS in the mitochondria of phagocytic cells to prevent inflammatory stimuli, such as host defense against bacterial and fungal infections [36]. 10^{-5}-10^{-2} M is usually regarded as a safe hypochlorite concentration range, outside of which may bring about many health risks like neural degeneration, cardiovascular disease and even cancers [37-42]. Considering real-time and in-situ detection, we speculate that traditional options, potentiometric titration and electrochemical analysis, for detection of ClO^- are not the best methods since both of which need complex sample preparation, expensive and complicated instruments and long response time. That is the main reason we take fluorescent chemo-sensors into consideration for their special advantages such as simplicity, low cost, high sensitivity, high selectivity, and rapid response time [43-47].

Fluorescence sensing for real-time visual detection of hypochlorite (ClO^-) in vitro and in vivo has been a hot topic among researchers in recent decades. In 2014, Yin and Yang et al. found a commercially available fluorescent reagent that be used as hypochlorite probe. Based on the idea of oxidizing amino groups to imines, they noticed fluorescent emission of probe changed from blue to green in ethanol when hypochlorite solution added [48]. One year later, Wang et al. designed and synthesized an ‘off-on’detection probe for the imaging of hypochlorous acid in mitochondria with a relatively long emission wavelength and detection limit was as low as 17.9 nM in PBS (containing 0.5% DMSO) [49]. In 2017, Huo’s group designed a probe to detect ClO^- in tap and river water samples by spiking a known amount of standard ClO^-. Fluorescence quantum yield increased from 0.0008 to 0.112 when adding hypochlorite to non-fluorescent solution (DMSO: H_2O, v/v, 1/3) [50]. Recently, many scholars have extended the research of molecular probes to the fields of biology and biological applications [51] and cell imaging materials [52] as well as simultaneous the detection of endogenous hypochlorous acid [53-55]. In order to accurately tracking HClO formation, efficient

and effective sensors for real-time monitoring in vivo are imperatively needed. However, most of the existing probes for HClO detection are poorly soluble in water and require additional organic solvent when used which is inapplicable in living cells [56-58]. Therefore, it is an urgent demand to unearth new indicators for highly sensitive and accurate detection of ClO^- in cells and organs.

Herein, we explored a o-hydroxyl aldehyde structure based naphthalimide derivative, named 2-butyl-6-hydroxy-1,3-dioxo-2,3-dihydro-1H-benzo[de]isoquinoline-5-carbaldehyde (**BHC**) that brought a hydroxyl and an aldehyde to equip naphthalimide core with a proton acceptor and donor and built a structure that increased the water solubility of organic compound. **BHC** showed a special selective response to ClO^- among kinds of common ions. The photoluminescence (PL) intensity and peak wavelengths could be reversibly regulated by UV-vis light, and addition of ClO^- solution. Based on these results, we synthesized and characterized **BHC** that had both photochromic ability and recognition of hypochlorite in living cells. To the best of our knowledge, this bifunctional compound was a novel one with a color-changing behavior based on ESIPT between hydroxyl and aldehyde groups. It was not only a new breakthrough in anti-counterfeiting and optical imaging, but an efficient fluorescent probe for ClO^-. Moreover, this result will facilitate the development of smarter systems and functional compounds that integrate multiple switchable functions into a single molecule.

2 Experimental

2.1. Materials and Instrument

Reagents and solvents involved in the experiments were purchased online (AR grade) and there was no further purification unless mentioned. The use of deionized water was default in all aqueous operations and sample preparation. ^{1}H NMR and ^{13}C NMR spectra were collected on Bruker-600 MHz and Bruker-400 MHz spectrometer in Deuterated reagents with TMS as an internal standard. Mass spectra were obtained on a Bruker Ultraflextreme MALDI TOF/TOF mass spectrometer. UV-vis spectra were recorded on Shimadzu UV-3600 with a UV-VIS-NIR spectrophotometer. Emission spectra were collected by a HITACHI fluorescence spectrometer (F-4600). The ground state geometries of all molecules were fully optimized using density functional theory (DFT) at the B3LYP/6-31G (d, p) level, as implemented in Gaussian 09W software package. The cell imaging

experiments were carried out by using Confocal Scanning Microscopy (Leica, TCS sp5 II).

2.2. Synthesis

2.2.1 Synthesis of 6-bromo-2-butyl-1H-benzo[de]isoquinoline-1,3(2H)-dione (a)

4-Bromo-1,8-naphthalic anhydride (1.385 g, 5 mmol) and n-butylamine(0.438 g, 6 mmol) were dissolved in ethanol(30 ml) and refluxed for about 5 hours. The reaction was monitored by TCL until the end of the reaction. After cooling to room temperature, white product was obtained by recrystallization, 1.494 g. Yield: 90%. ^{1}H NMR (600 MHz, $CDCl_3$) δ 8.68 (dd, *J* = 7.3, 0.8 Hz, 1H), 8.58 (dd, *J* = 8.5, 0.8 Hz, 1H), 8.43 (d, *J* = 7.8 Hz, 1H), 8.06 (d, *J* = 7.8 Hz, 1H), 7.87 (dd, *J* = 8.3, 7.4 Hz, 1H), 4.30 – 4.06 (m, 2H), 1.74 (tt, *J* = 7.7, 6.7 Hz, 2H), 1.52 – 1.41 (m, 2H), 1.00 (t, *J* = 7.4 Hz, 3H). ^{13}C NMR (151 MHz, $CDCl_3$) δ 163.65 (d, *J* = 3.5 Hz), 133.23 (s), 132.03 (s), 131.22 (s), 131.10 (s), 130.64 (s), 130.20 (s), 129.02 (s), 128.09 (s), 123.18 (s), 122.31 (s), 40.40 (s), 30.18 (s), 20.39 (s), 13.86 (s). TOF-MS (ESI) m/z calcd. For $C_{16}H_{14}BrNO_2$ $[M+H]^+$: 332.0208, found: 332.0200.

2.2.2 Synthesis of 2-butyl-6-methoxy-1H-benzo[de]isoquinoline-1,3(2H)-dione (b)

Compound **a** (0.996 g, 3 mmol), sodium methoxide (0.648 g, 12 mmol), and $CuSO_4 \cdot 5H_2O$ (0.14 g, 0.6 mmol) were dissolved in 50ml methanol. The reaction was protected under a nitrogen atmosphere and was refluxed for about 8 hours to the end. When cooling to room temperature, the solvent was removed by rotary evaporation and the concentrated product was purified by silica gel flash column chromatography (dichloromethane (DCM)/hexane (Hex) (1/3, v/v) as the eluent) to get a yellow-green product, 0.64 g. Yield: 75%. ^{1}H NMR (600 MHz, $CDCl_3$) δ 8.60 (d, *J* = 7.2 Hz, 1H), 8.55 (dd, *J* = 8.3, 2.0 Hz, 2H), 7.74 – 7.65 (m, 1H), 7.04 (d, *J* = 8.3 Hz, 1H), 4.20 – 4.16 (m, 2H), 4.14 (s, 3H), 1.77 – 1.65 (m, 3H), 1.51 – 1.42 (m, 2H), 0.99 (t, *J* = 7.4 Hz, 3H). ^{13}C NMR (151 MHz, $CDCl_3$) δ 164.57 (s), 164.02 (s), 160.78 (s), 133.42 (s), 131.53 (s), 129.39 (s), 128.59 (s), 125.95 (s), 123.51 (s), 122.50 (s), 115.20 (s), 105.18 (s), 56.20 (s), 40.12 (s), 30.29 (s), 20.43 (s), 13.89 (s). TOF-MS (ESI) m/z calcd. For $C_{17}H_{17}NO_3$ $[M+H]^+$: 284.1208, found: 284.1233.

2.2.3 Synthesis of 2-butyl-6-hydroxy-1H-benzo[de]isoquinoline-1,3(2H)-dione (c)

Compound **b** (0.566 g, 2 mmol) was added into 20 ml hydro-bromic acid, and an appropriate amount of glacial acetic acid was put into the flask to increase the solubility. The reaction was refluxed for 12 hours under a nitrogen atmosphere and was tracked to the end by TCL. After cooling, the solution was poured into ice water and filtered. The crude product was purified with

silica gel column chromatography (dichloromethane (DCM)/hexane (Hex) (2/1, v/v) as the eluent) to obtain a pale green product, 0.269 g. Yield: 47.5%. ^{1}H NMR (600 MHz, DMSO) δ 11.87 (s, 1H), 8.65 – 8.05 (m, 3H), 7.46 (ddd, *J* = 12.7, 11.4, 6.0 Hz, 2H), 3.35 (s, 2H), 1.60 (dd, *J* = 14.2, 6.7 Hz, 2H), 1.41 – 1.16 (m, 2H), 1.11 – 0.64 (m, 3H). ^{13}C NMR (151 MHz, DMSO) δ 164.17 (s), 163.50 (s), 160.72 (s), 134.06 (s), 131.64 (s), 129.67 (s), 129.38 (s), 126.13 (s), 122.87 (s), 122.31 (s), 113.11 (s), 110.45 (s), 55.39 (s), 30.23 (s), 20.29 (s), 14.21 (s). TOF-MS (ESI) m/z calcd. For $C_{16}H_{15}NO_3$ $[M+H]^+$: 270.1052, found:270.1010.

2.2.4 Synthesis of 2-butyl-6-hydroxy-1,3-dioxo-2,3-dihydro-1H-benzo[de]isoquinoline -5-carbaldehyde (BHC)

Compound **c** (269 mg, 1 mmol) and magnesium chloride (140.85 mg, 1.5 mmol) were dissolved in acetonitrile (15 ml), trimethylamine (404 mg, 4 mmol) was dropped during stirring, and paraformaldehyde (6.8mmol) was added in the heating process. The reaction was refluxed for 4 h and was monitored by TCL until finished completely. The mixture solution was adjusted to weak acidity with 5% dilute hydrochloric acid and the solution was extracted with DCM several times. The combined organic extracts were dried with $MgSO_4$, then filtered, concentrated under vacuum. The residue was purified with silica gel column chromatography (dichloromethane (DCM)/hexane (Hex) (1:1, v/v) as the eluent), and 195 mg product was collected. Yield: 65%. ^{1}H NMR (600 MHz, $CDCl_3$) δ 13.21 (s, 1H), 10.46 – 9.73 (m, 1H), 8.76 (dd, *J* = 8.8, 7.2 Hz, 3H), 7.84 (t, *J* = 7.8 Hz, 1H), 4.44 – 3.77 (m, 2H), 1.91 – 1.24 (m, 5H), 1.00 (t, *J* = 7.4 Hz, 3H). ^{13}C NMR (151 MHz, $CDCl_3$) δ 196.47 (s), 165.77 (s), 163.76 (s), 163.10 (s), 134.94 (s), 134.17 (s), 131.86 (s), 130.40 (s), 127.08 (s), 122.92 (d, *J* = 8.3 Hz), 115.07 (d, *J* = 36.8 Hz), 53.45 (s), 40.33 (s), 30.21 (s), 20.38 (s), 13.86 (s).TOF-MS (ESI) m/z calcd. For $C_{17}H_{15}NO_4$ $[M+H]^+$: 298.1001, found: 298.1013.

2.3 The preparation of various analytes

A stock solution of BHC (1.0 mM) was prepared in tetrahydrofuran (THF). The working standard solutions were prepared by diluting the stock solution to 10 μM by PBS buffer (pH = 7.4). The sodium hypochlorite (NaClO) solution was prepared by diluting the 14% commercially purchased NaClO, hydrogen peroxide (H_2O_2) was prepared by diluting the 35% (w/w) purchased one, and all ions are obtained by dissolving the corresponding salt in distilled water.

2.4 Cell cultures

HeLa cells were cultured on glass-bottom Dulbecco's modified eagle media (DMEM) culture dishes which were supplemented with 10% (v/v) fetal bovine serum (FBS). 100μg mL^{-1} penicillin–streptomycin and were set in a humidified 37 °C incubator containing 5% CO_2. For the detection of exogenous ClO^-, the HeLa cells were incubated with BHC (10 μM) for 30 mins at 37 °C and washed with PBS buffer three times, and then added fresh prepared ClO^- (5 μM) solution in culture media and stay for 30 mins. For the detection of endogenously produced ClO^-, the HeLa cells were incubated with **BHC** (10 μM) for 30 mins at 37 °C incubator, and then washed with PBS buffer three times before being stimulated by 2 ug/mL lipopolysaccharides (LPS) and phorbol 12-myristate 13acetate (PMA) for 2 hours. As a control experiment group, the HeLa cells were incubated with BHC (10 μM) for 30 mins at 37 °C incubator, and then washed with PBS buffer three times, then stimulated with 200 μM 4-aminobenzoic-acid-hydrazide(ABH) and 2 ug/mL lipopolysaccharides (LPS) and phorbol 12-myristate 13 acetate (PMA) for 2 hours.

3. Results and discussions

3.1 Synthesis and characterization

The synthetic procedure for compound **BHC** was illustrated in Scheme 1 using 4-Bromo-1,8-naphthalic anhydride as the starting material. Firstly, compound **a** was conveniently prepared in high yield in ethanol. Then, intermediate **a** was effectively transformed into **b** in the presence of CH_3ONa, $CuSO_4{\cdot}5H_2O$ in methanol under N_2 protection. Third, compound **c** was directly synthesized in a high yield by a simple reduction reaction. At last, compound **c** reacted with the paraformaldehyde in acetonitrile to give the **BHC**, which was a new method used in this article. The raw **BHC** was purified through column chromatography (Yield : 65%) and was structurally characterized by ^{1}H-NMR, ^{13}C-NMR, and MALDI TOF/TOF mass spectrometer techniques. In a word, compound **BHC** had been efficiently synthesized in relatively high yield and a new and simple synthetic method

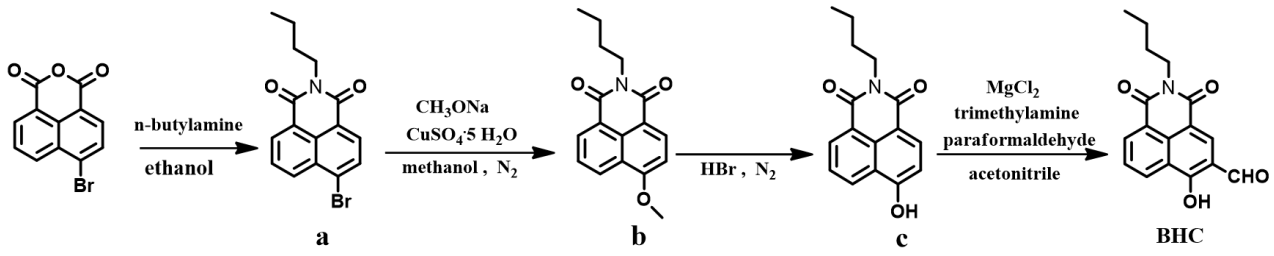

Scheme 1 Synthetic routes of compound **BHC**

3.2 Photochromic properties

3.2.1 The reversible photochromic properties of BHC

The absorption and photoluminescence (PL) spectra of the solid **BHC** before and after UV irradiated were recorded in Fig.1. It could be seen that the absorption of **BHC** after **UV** irradiation was remarkably enhanced between 425 nm and 475 nm, which means an extension of the conjugated structure caused by the change of the enol to the trans-keto structure. There were two emissions in the PL spectrum, one at 462 nm and the other at 546 nm. After intense ultraviolet excitation at 390 nm, a sharp decrease in the fluorescence intensity at 464 nm were observed in Fig.1b. The former was the fluorescence of **BHC** itself and the latter might caused by the excited state intramolecular proton transfer of some compounds (ESIPT). Under excitation at 390 nm, most of the compounds converted to the trans-keto structure, and intramolecular push-pull electron effect was greatly attenuated while electron-withdrawing ability of the ketone structure was prominent. The initial state of **BHC** exists in the structure of enol and after being excited with higher energy ultraviolet light, proton transferred from hydroxyl to aldehyde (Scheme 2). Such movement is reversible, and the initial enol can be achieved again under long wavelengths of light and heating condition. The UV absorption and fluorescence spectra were mutually confirmed, indicating the fact that **BHC** has experienced the process from an enol form to a trans-keto one.

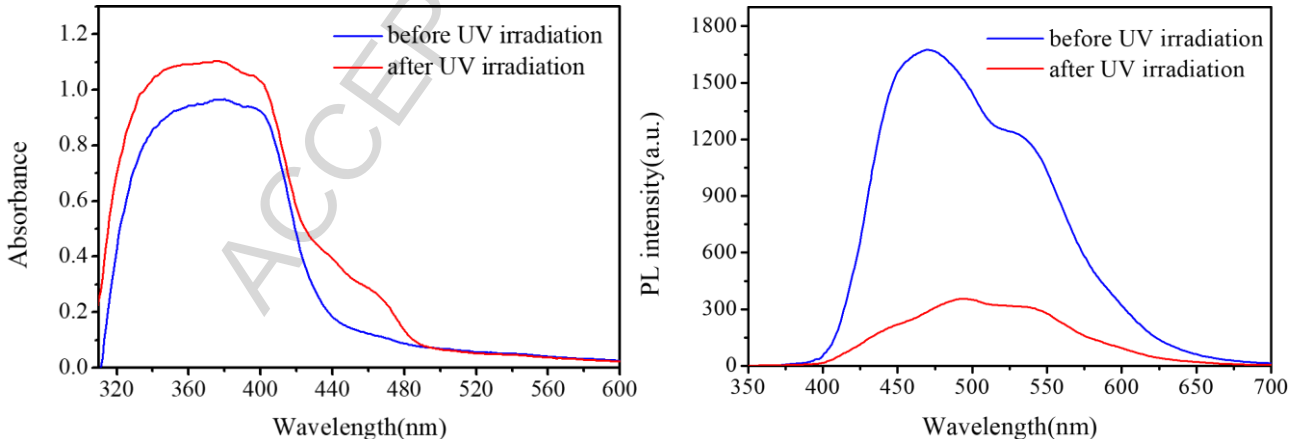

(a) (b)

Fig. 1. (a) The UV–vis absorption spectra of BHC before and after UV irradiation in solid state (b) The PL spectra of of **BHC** before and after UV irradiation in solid state (λ_{ex} = 390 nm, λ_{em} = 462 nm, 546 nm, slit: 5 nm/5 nm).

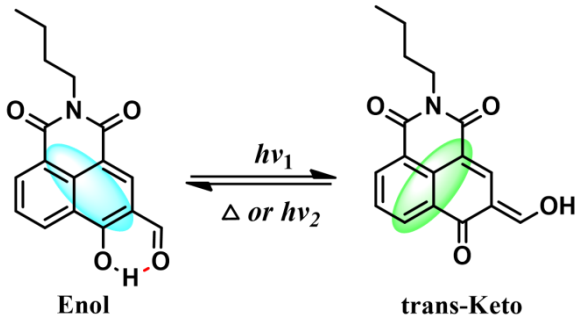

Scheme 2 Photochromic mechanism of **BHC** upon UV irradiation

In addition to the above photochromic properties, the solid trans-keto compounds also exhibited thermal fading and photo bleaching properties, and the results are shown in the Fig.2. In daylight, the white compound turns yellow after exposure to ultraviolet light for 20 seconds and then returns to milky white when heating or irradiate with intense white light. At the same time, the fluorescence changes from light blue to deep yellow, again returning to the initial state under the 'washing' of heat and light. The compound not only shows a time-dependent fading rate, but also exhibits thermal fading ability. Specifically, the rate of fading is positively correlated with temperature. As shown in the Fig.2b, the slope of the fitted line, absorption intensity at 409 nm as the ordinate and time as the abscissa, is -0.00607 for 65 ℃, which is twice of that of 25 ℃ (0.00392). The data under 25 ℃, 45 ℃, 65 ℃ fully demonstrate the relationship between fading rate and temperatures, which has a great guiding effect on the application range of compound (Fig.S2).

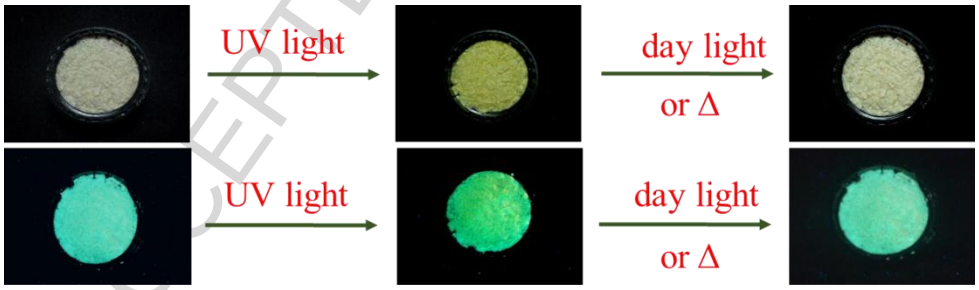

(a)

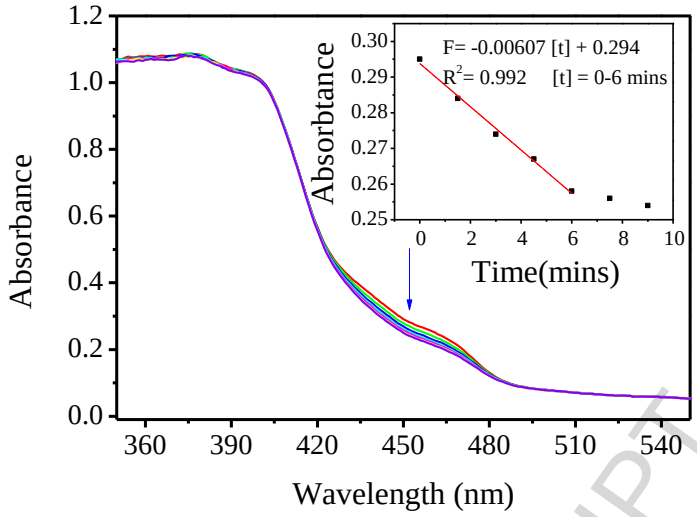

(b)

Fig. 2. (a) Photographs of **BHC** before and after photochromism, and photos after long-wavelength illumination or heating. (b) The thermal fading kinetics of **BHC** at 65 ℃.

3.2.2 Theoretical calculation

DFT calculations of **BHC** Enol and trans-Keto were performed on the B3LYP/6-31G* level to gain a deeper understanding of the photochromic properties (Fig. 3a). Theoretically, the energy gap (EG) between HOMO and LUMO was related to the absorption wavelength: a smaller EG was conducive to electron transport, causing a red-shift in absorption wavelength. As expected, Enol's EG was 3.778 ev and trans- Keto's EG was 3.416 ev (Fig. 3a), which was very consistent with the red-shifted absorption wavelength in Fig. 1a. The trend that HOMO and LUMO of trans-keto shifting to the carbonyl moiety confirmed the electron-withdrawing property of the carbonyl moiety. It also suggested that **BHC** photochromism was caused by the absorption of energy from UV irradiation. As a photochromic material, its fatigue resistance and erasability were properties that need to be studied. The fatigue resistance of BHC was investigated by repeatedly switching light conditions for five times. As shown in the Fig.3b, the fluorescence remained almost constant without degradation, and the pattern written on the tiled compound by a laser pointer intuitively reflected discoloration process, indicating good fatigue resistance of **BHC**. Reversible photochromic properties and good fatigue resistance, small degree of color change indicated its potential to become an novel anti-counterfeiting material with higher secrecy coefficient or decorative material, and its commercial production application is promising.

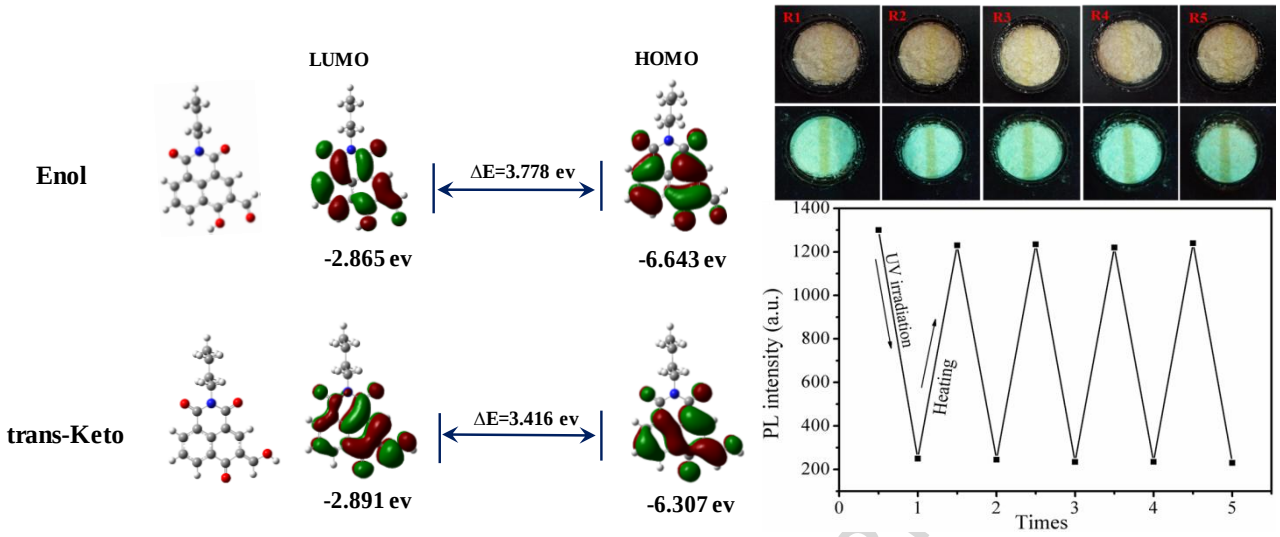

Fig.3. (a) Frontier molecular orbital amplitude plots and energy levels of the HOMOs and the LUMOs of BHC Enol and trans-Keto. (b)The modulation of the FL intensity of BHC at 546 nm as a result of alternating irradiation and heating treatment.

3.3 Hypochlorite (ClO^-) Detection properties

3.3.1 Photoluminescence and UV–vis spectra in water solution

The UV absorption and photoluminescence (PL) spectra of the compound in a complete PBS solution were shown in Fig.4a. The maximum absorption is around 409 nm and the maximum emission is around 510 nm, which results in strong yellow-green fluorescence (365nm handheld UV light) and a large Stokes shift. The PL quantum yield of the compound BHC is as high as 32.06% which is a relatively higher PL quantum yield compared to other water-soluble dyes. As shown in Fig. 4b, with sodium hypochlorite solution dropped, the PL of solution quenched from bright green to colorless, which facilitates visual inspection of the test results.

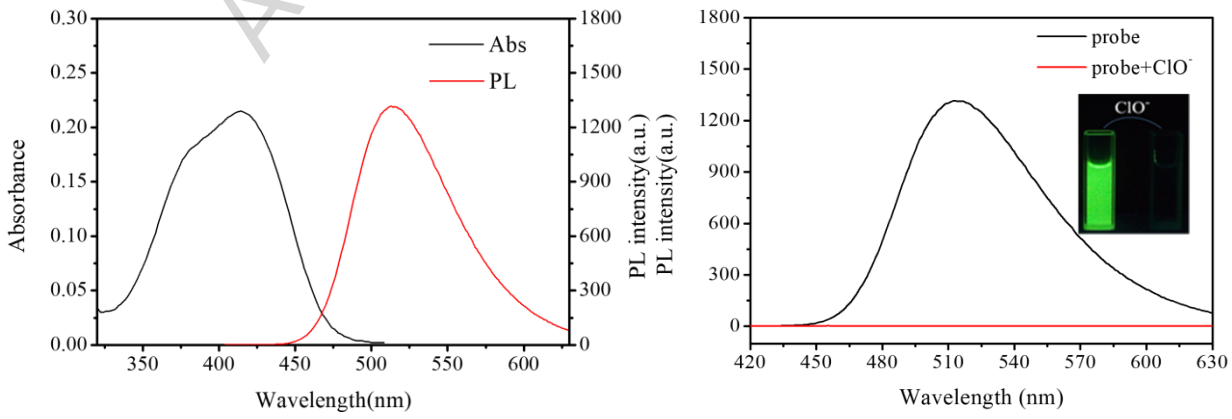

(a) (b)

Fig.4. (a) The UV–vis absorption spectra and photoluminescence (PL) spectra of BHC (10 μM) in PBS buffer solution (pH 7.4). (b) The PL spectra of probe **BHC** (10 μM) in the presence of ClO^- (50 μM) in PBS buffer solution (pH 7.4) (λ_{ex} = 409 nm, λ_{em} = 510 nm, slit: 5 nm/5 nm).

3.3.2 Selectivity

In order to evaluate the hypochlorite selectivity of the probe, the photoluminescence (PL) spectra of PBS buffered solution containing the probe and the analytes (100 equiv.) were recorded in Fig.5 and were used to study the possible effects of other analytes posed on the probe. The results showed that all the analytes such as Ba^{2+}, Ca^{2+}, K^+, Mg^{2+}, Na^+, Zn^{2+}, Br^-, Cl^-, ClO_4^-, F^-, I^-, HS^-, NO_2^-, NO_3^-, SO_4^{2-}, H_2O_2, PF_6^-, CN^-, AcO^- did not significantly shade the PL of the solution. When ClO^- was added, the PL quenched quickly. Moreover, for the purpose of exploring the effect of the probe on the competitive recognition of ClO^-, ClO^- being added into the mixed solution in the presence of multiple ions, the results showed that the recognition effect was still quite optimistic (as shown in Fig. 5b). A good selectivity for ClO^-among various analytes were exhibited through above experiments.

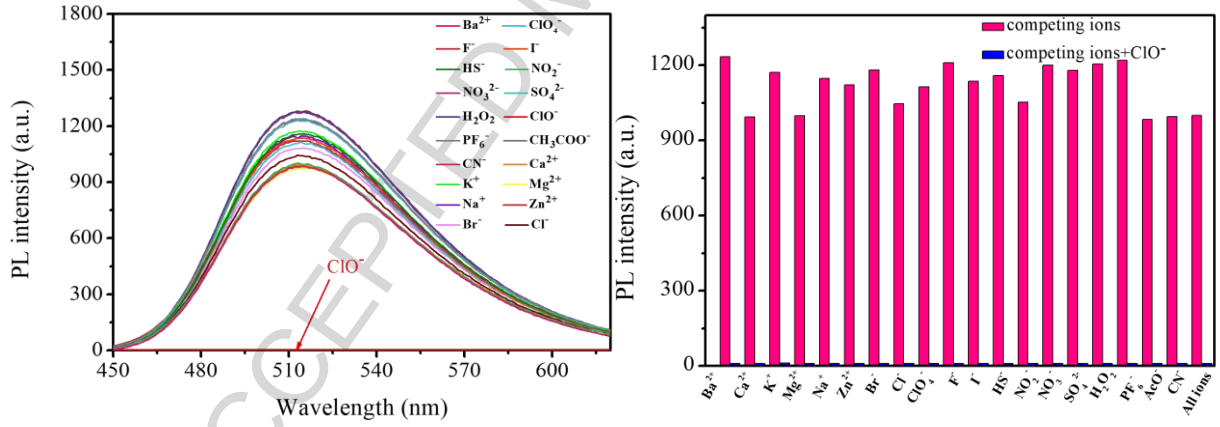

(a) (b)

Fig.5. (a), (b) The photoluminescence (PL) spectra of probe (10 μM) with various analytes (50 μM for ClO^- and 100 μM for other analytes) in PBS buffer solution (λex = 409 nm, λem = 510 nm, slit: 5 nm/5 nm pH 7.4).

3.3.3 pH dependent

The effect of different pH on the identification of ClO^- was analyzed. Photoluminescence (PL) intensity of the probe and probe with ClO^- at different pH conditions were recorded in Fig.6. In the pH range of 1-4, the PL of probe is very weak. As is known to all, ClO^- is not stable in strongly acidic solutions. Therefore, the detection results in the pH range of 1-4 are negligible. When pH

exceeds 10, the OH^- in the alkaline solution largely hinders direct contact between protons on the hydroxyl group and ClO^- and the solution only shows the photoluminescence (PL) of the probe. Therefore, the probe covers the physiological pH range (5-9), which brings great application prospects.

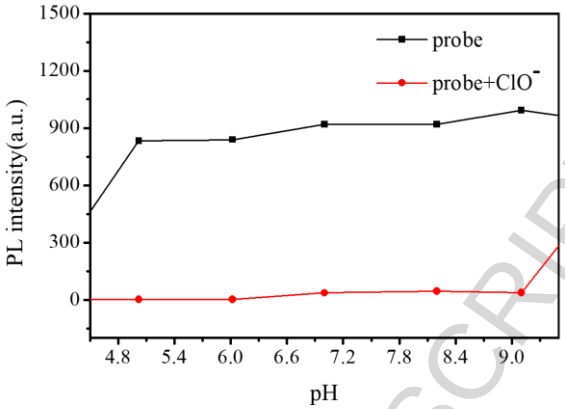

Fig.6. Effect of the pH on the photoluminescence (PL) intensity of probe alone and probe reacted with ClO^- (10 equiv) at different pH (4.5-9.5) (λex = 409 nm, λem = 510 nm, slit: 5 nm/5 nm).

3.3.4 The detection limit of probe for ClO^-

The detection limit of the probe is 1.16×10^{-8} M, which was calculated by the formula:

Detection limit=**3σ/k,** where **σ** is the standard deviation of blank sample, **k** is the slope between the fluorescence intensity ($I_{510\ nm}$) and the concentration of ClO^-. The fluorescence emission spectra of the probe (10 μM) were measured 11 times to obtain the standard deviation of the blank sample. The fluorescence spectra of probe with different equivalent amounts of ClO^- (0 eq-10 eq) was recorded 20 seconds after addition (Fig.7a) and the fluorescence intensity at 510 nm was taken as the ordinate, and the concentration of ClO^- was plotted on the abscissa, fitting a straight line (Fig. 7b).

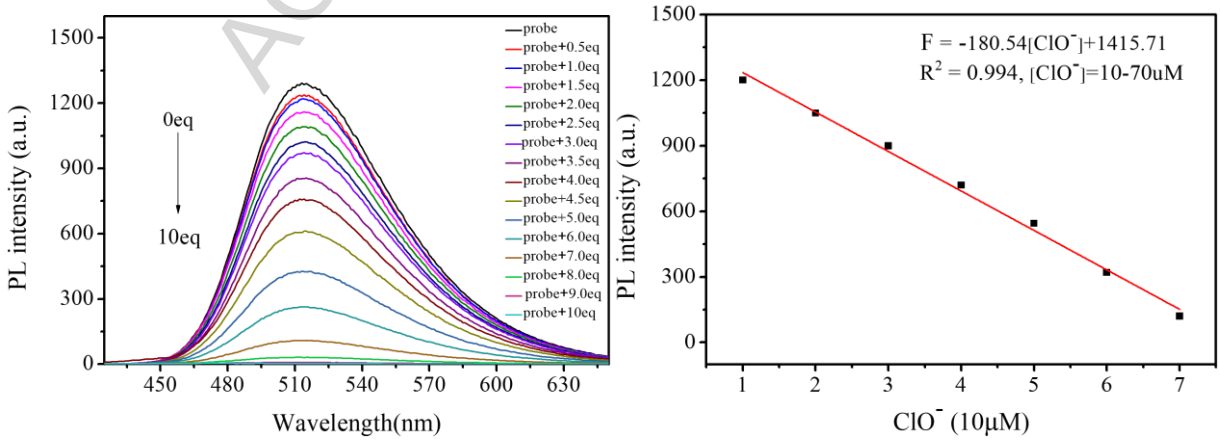

(a) (b)

Fig.7. (a) The photoluminescence (PL) spectra of probe (10 μM) in the presence of various concentrations of ClO^- (0-10 eq) in PBS buffer solution (λex = 409 nm, λem = 510 nm, slit: 5 nm/5 nm). (b) Plot of the photoluminescence (PL) intensity of probe at 510 nm as a function of the concentration of ClO^- (λex = 409 nm).

3.3.5 Proposed mechanism

Based on reasonable and reliable characterization of ^{1}H NMR, the probe detection mechanism was as shown in Figure.8. The oxidation of hypochlorous acid prompts us to conjecture that the phenolic hydroxyl group was oxidized to aryl ketone, therefore, a crude color reaction were performed. An aqueous solution of ferric chloride was added to the probe solution with no hypochlorous acid and the solution was dark purple-red. However, when ferric chloride solution was added to the solution to which sodium hypochlorite had been added before, there was no noticeable discoloration, which initially demonstrated conversion of the phenolic hydroxyl group. In order to figure out exact recognition mechanism of the probe, hypochlorous acid was titrated to deuterated reagents with dissolved probes and ^{1}H NMR shows an obvious disappearance of phenolic hydroxyls (Fig.S3†.). This indicates that hypochlorite oxidation probes only oxidize hydroxyl groups to carbonyl groups.

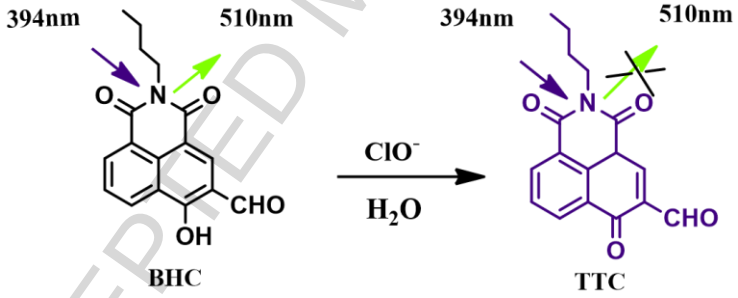

Fig.8. The proposed mechanism of the probe **BHC** sensing ClO^-.

3.3.6 Cellular imaging

Considering the excellent water solubility and bright fluorescence as well as the recognition for ClO^-, the potential applications in the field of cell imaging and exogenous ClO^- detection were further explored. Fluorescence imaging experiments were performed in living HeLa cells who were set on 6-well plates with **BHC** and adhere for 24 hours. The cells were washed three times with PBS buffer solution before the experiment. Firstly, four groups of cells were incubated with 10 μM **BHC** aqueous solution in a 37 °C incubator for 30 minutes and then washed three times with PBS buffer solution. When the probe alone incubated the cells, they presented bright fluorescence under the green channel (as shown in Fig.9.A). However, when exogenous hypochlorous salt was added to

the medium for 30 minutes, the fluorescence disappeared because the probe reacted with hypochlorous acid and Intramolecular charge transfer mechanism in molecule was broken (as shown in Fig.9.B). In the process of tracking cell endogenous hypochlorous acid, pretreated cells were stimulated with lipopolysaccharides (LPS) and phorbol 12-myristate 13 acetate (PMA) to give some hypochlorous acid. Similarly, it was observed that the fluorescence of the cells was shut down, indicating that the probe is able to monitor ClO^- successfully (as shown in Fig.9.C). As a comparative experiment, aside from LPS and PMA, ABH was added to inhibit the production of hypochlorous acid in cells and it was found that the fluorescence of the cells did not disappear (as shown in Fig.9.D).

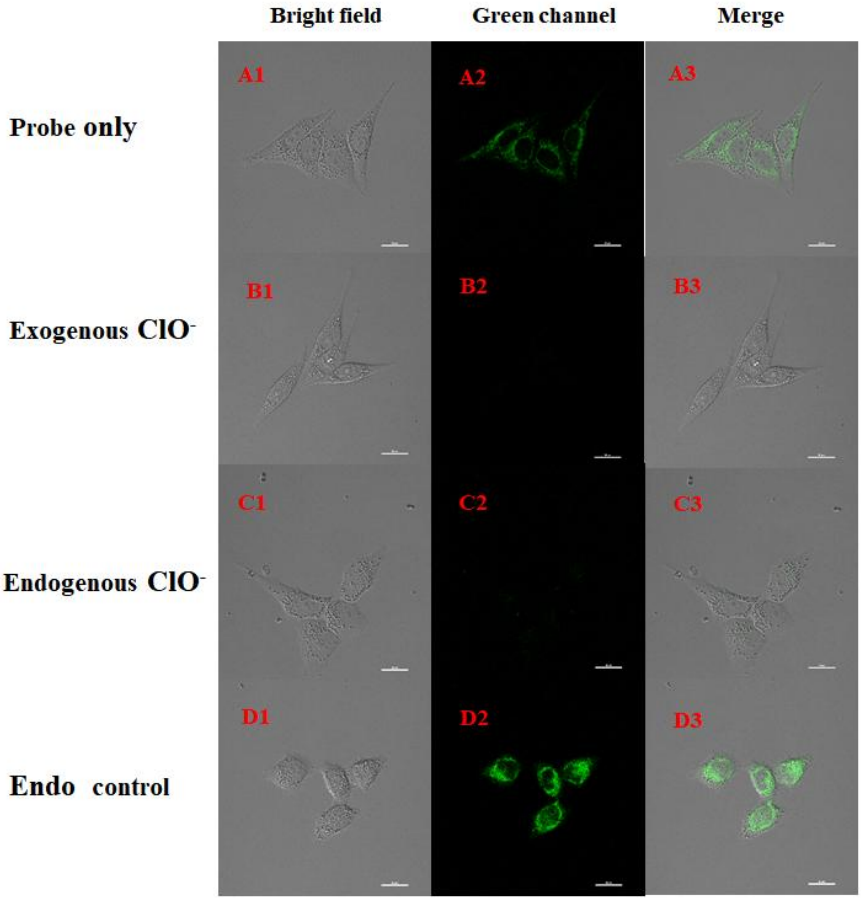

Fig.9. Confocal fluorescent image of HeLa cells. (A1-3) Fluorescent image of cells incubated with probe (10 μM) for 30 mins under bright field, green channel and the merge respectively. (B1-3) Fluorescent image of cells treated with probe (10 μM) and then treated with ClO^- (5 μM) for 30 mins. (C1-3) Fluorescent image of cells treated with probe (10 μM) and then treated with LPS and PMA(2 ug/mL) for 30 mins under bright field, green channel and the merge respectively. (D-3) Fluorescent image of cells treated with probe (10 μM) and then treated with ABH,

LPS and PMA(2 ug/mL) for 30 mins under bright field, green channel and the merge respectively.

At the same time, the toxicity and photoluminescence (PL) stability of the probe in cells were discussed. After 8 hours of incubation with different concentrations of probe, cell survival rate remained high and the photoluminescence intensity within 8 minutes was also relatively stable (Fig.10). Therefore, from the above analysis and experiments, it could be seen that the probe can not only stain cells, but also accurately track the generation of hypochlorous acid in vivo and in vitro, thus broadening the path for cell imaging and biological applications.

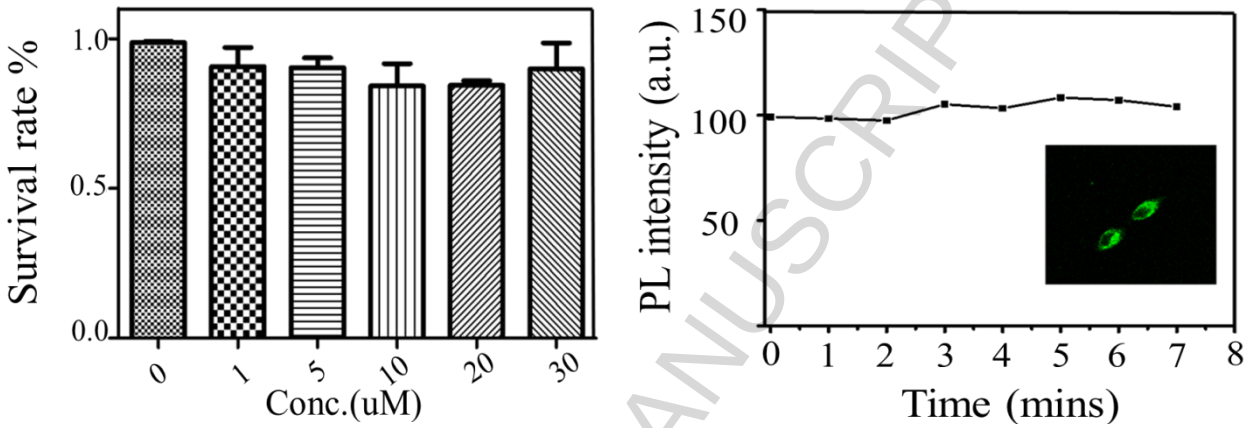

(a) (b)

Fig.10. (a) The survival rate of cells cultured with different probe concentrations (0-30 μm) for 8 hours. (b) Stained cell photoluminescence (PL) intensity versus time in 8 mins.

4. Conclusion

In summary, a bifunctional, water-soluble **BHC** has been synthesized, presenting a photoswitch ability that responding to ClO^- and alternating UV/vis light irradiation. **BHC** shows a reversible photochromic behavior, good fatigue resistance and adjustable bleaching rate, which broadens choice of smart switching and anti-counterfeiting marking materials. The selectivity to hypochlorite at physiological pH makes it suitable for cell imaging and ClO^- detection in vitro and vivo. It has been proved non-toxic by cell cultivation test and bright green to no fluorescence detection result is easy to identify. The practical applications of probe such as imaging living cells and the detecting of hypochlorite in vivo were confirmed by cell culture experiments. The detection limit was as low as 1.16×10^{-8} M. This dual functional compound is not only a new breakthrough in anti-counterfeiting and optical imaging, but also a practical fluorescent probe for ClO^-, which provides evidence for the idea of integrating multiple functions into one molecule.

Acknowledgements

This work was supported by the Fundamental Research Funds for the Central Universities (2019XKQYMS72) and the Priority Academic Program Development of Jiangsu Higher Education Institutions.

References

[1] L. Ma, S. Wang, C. Li, D. Cao, T. Li, X. Ma, Photo-controlled fluorescence on/off switching of a pseudo[3]rotaxane between an AIE-active pillar[5]arene host and a photochromic bithienylethene guest, Chem. Commun. 54 (2018) 2405-2408. https://doi.org/10.1039/c8cc00213d.

[2] W. Zeng, H.Y. Lai, W.K. Lee, M. Jiao, Y.J. Shiu, C. Zhong, S. Gong, T. Zhou, G. Xie, M. Sarma, Achieving Nearly 30% External Quantum Efficiency for Orange-Red Organic Light Emitting Diodes by Employing Thermally Activated Delayed Fluorescence Emitters Composed of 1,8-Naphthalimide-Acridine Hybrids, Adv. Mater. 30 (2018) 1704961 (1-8). https://doi.org/10.1002/adma. 201704961.

[3] Z-M. Zhang, B-X. Miao, X-X. Tang, Z-H. Ni, A series of 4,5,9,10-tetrahydropyrene-based tetraarylethenes: synthesis, structures and solid-state emission behavior, Rsc Adv. 8 (2018) 15173-15180. https://doi.org/10.1039/c8ra00057c.

[4] H. Sun, X-X. Tang, B-X. Miao, Y. Yang, Z-H Ni, A new AIE and TICT-active tetraphenylethene-based thiazole compound: Synthesis, structure, photophysical properties and application for water detection in organic solvents, Sensors Actuators B. 267 (2018) 448–456. https://doi.org/10.1016/j.snb.2018.04.022.

[5] Z. Li, X. Zhang, S. Wang, Y. Yang, B. Qin, K. Wang, T. Xie, Y. Wei, Y. Ji, Polydopamine coated shape memory polymer: Enabling light triggered shape recovery, light controlled shape reprogramming and surface functionalization, Chem. Sci. 7 (2016) 4741–4747. https://doi.org/10.1039/c6sc00584e.

[6] L. Gai, J. Mack, H. Liu, Z. Xu, H. Lu, Z. Li, A BODIPY fluorescent probe with selective response for hypochlorous acid and its application in cell imaging, Sensors Actuators B. 182 (2013) 1-6. http://dx.doi.org/10.1016/j.snb.2013.02.106.

[7] A.O. Eseola, H. Görls, M. Bangesh, W. Plass, ESIPT-capable 2,6-di(1H-imidazol-2-yl)phenols with very strong fluorescent sensing signals towards Cr(iii), Zn(ii), and Cd(ii): molecular variation effects on turn-on efficiency, N. J. Chem. 42 (2018) 7884-7900. https://doi.org/10.1039/c8nj01265b.

[8] L. Hou, X. Kong, Y. Wang, J. Chao, C. Li, C. Dong, Y. Wang, S. Shuang, An anthraquinone-based highly

selective colorimetric and fluorometric sensor for sequential detection of Cu^{2+} and S^{2-} with intracellular application, J. Mater. Chem. B. 5 (2017) 8957-8966. https://doi.org/10.1039/c7tb01596h.

[9] K.N. Hearn, T.D. Nalder, R.P. Cox, H.D. Maynard, T.D.M. Bell, F.M. Pfeffer, T.D. Ashton, Modular synthesis of 4-aminocarbonyl substituted 1,8-naphthalimides and application in single molecule fluorescence detection, Chem. Commun. 53 (2017) 12298-12301. https://doi.org/10.1039/c7cc07922b.

[10] P. Kumari, S.K. Verma, S.M. Mobin, Water soluble two-photon fluorescent organic probes for long-term imaging of lysosomes in live cells and tumor spheroids, Chem. Commun. 54 (2018) 539-542. https://doi.org/10.1039/c7cc07812a.

[11] L. Tan, S. Mo, B. Fang, W. Cheng, M. Yin, Dual fluorescence switching of a Rhodamine 6G-naphthalimide conjugate with high contrast in the solid state, J. Mater. Chem. C. 6 (2018) 10270-10275. https://doi.org/10.1039/c8tc03654c.

[12] M. Tomasulo, S. Giordani, F.M. Raymo, Fluorescence Modulation in Polymer Bilayers Containing Fluorescent and Photochromic Dopants, Adv. Funct. Mater. 15 (2010) 787-794. https://doi.org/10.1002/adfm.200400381.

[13] Y. Inagaki, K. Mutoh, J. Abe, Stepwise photochromism of bisnaphthopyrans exhibiting an excitation intensity-dependent color change, Photochem. Photobiol. Sci. 17 (2018) 946-953. https://doi.org/10.1039/c8pp00205c.

[14] K. Watanabe, T. Ubukata, Y. Yokoyama, Photochromism and the fluorescence properties of bisbenzothienylethene and S,S,S′,S′-tetraoxide derivatives with dual conjugated fluorescent groups on their side chains, Photochem. Photobiol. Sci. 17 (2018) 711-717. https://doi.org/ 10.1039/c8pp00050f.

[15] H. Tian, B. Qin, R. Yao, X. Zhao, S. Yang, A Single Photochromic Molecular Switch with Four Optical Outputs Probing Four Inputs, Adv. Mater. 15 (2003) 2104-2107. https://doi.org/10.1002/adma.200305425.

[16] R. François, N.A. D., H. Florence, T. Bernard, R. Raphaël, W. Johan, G. Yann, Engineering Solid-State Molecular Switches: N-Salicylidene N-Heterocycle Derivatives, Eur. J. Org. Chem. 2010 (2010) 621-637. https://doi.org/10.1002/ejoc.200901175.

[17] L. Chen, J. Zhang, Q. Wang, L. Zou, Photo-controllable and aggregation-induced emission based on photochromic bithienylethene, Dyes Pigments. 123 (2015) 112-115. https://doi.org/10.1016/j.dyepig.2015.07.031.

[18] I. Yildiz, E. Deniz, F.M. Raymo, Fluorescence modulation with photochromic switches in nanostructured constructs, Chemin. 38 (2009) 1859-1867. https://doi.org/10.1039/b804151m.

[19] S.K. Sahoo, R.K. Bera, M. Baral, B.K. Kanungo, Excited state intramolecular proton transfer (ESIPT) in a

dioxotetraamine derived schiff base and its complexation with Fe(III) and Cr(III), J. Photochem. Photobiol. A. 188 (2007) 298-310. https://doi.org/10.1016/j.jphotochem.2006.12.027.

[20] K.J. Eon, P. Soo Young, Advanced organic optoelectronic materials: harnessing excited-state intramolecular proton transfer (ESIPT) process, Adv. Mater. 23 (2011) 3615-3642. https://doi.org/10.1002/adma.201102046.

[21] A. Brenlla, M. Veiga, J.L. Pérez Lustres, M.C. Ríos Rodríguez, F. Rodríguez-Prieto, M. Mosquera, Photoinduced Proton and Charge Transfer in 2-(2′-Hydroxyphenyl)imidazo[4,5-b]pyridine, J. Phys. Chem. B. 117 (2013) 884-896. https://doi.org/10.1021/jp311709c.

[22] L. Wang, Y. Li, X. You, K. Xu, Q. Feng, J. Wang, Y. Liu, K. Li, H. Hou, An erasable photo-patterning material based on a specially designed 4-(1,2,2-triphenylvinyl)aniline salicylaldehyde hydrazone aggregation-induced emission (AIE) molecule, J. Mater. Chem. C. 5 (2017) 65-72. https://doi.org/10.1039/c6tc03791g.

[23] J. Zhao, S. Ji, Y. Chen, H. Guo, P. Yang, Excited state intramolecular proton transfer (ESIPT): from principal photophysics to the development of new chromophores and applications in fluorescent molecular probes and luminescent materials, Phys. Chem. Chem. Phys. 14 (2012) 8803-8817. https://doi.org/10.1039/c2cp23144a.

[24] L. McDonald, J. Wang, N. Alexander, H. Li, T. Liu, Y. Pang, Origin of Water-Induced Fluorescence Turn-On from a Schiff Base Compound: AIE or H-Bonding Promoted ESIPT, J. Phys. Chem. B. 120 (2016) 766-772. https://doi.org/10.1021/acs.jpcb.5b10909.

[25] Y-T. Chen, P-J. Wu, C-Y. Peng, J-Y. Shen, C-C. Tsai, W-P. Hu, P-T. Chou, A study of the competitive multiple hydrogen bonding effect and its associated excited-state proton transfer tautomerism, Phys. Chem. Chem. Phys. 19 (2017) 28641-28646. https://doi.org/10.1039/c7cp05002j.

[26] S. Chaiwongwattana, D. Skalamera, N. Doslic, C. Bohne, N. Basaric, Substitution pattern on anthrol carbaldehydes: excited state intramolecular proton transfer (ESIPT) with a lack of phototautomer fluorescence, Phys. Chem. Chem. Phys. 19 (2017) 28439-28449. https://doi.org/10.1039/C7CP05472F.

[27] M. Saleem, K.H. Lee, Optical sensor: a promising strategy for environmental and biomedical monitoring of ionic species, RSC Adv. 5 (2015) 72150-72287. https://doi.org/10.1039/C5RA11388A.

[28] H. Nie, W. Yang, M. Yang, J. Jing, X. Zhang, Highly specific and ratiometric fluorescent probe for ozone assay in indoor air and living cells, Dyes Pigments. 127 (2016) 67-72. https://doi.org/10.1016/j.dyepig.2015.12.020.

[29] J-C. Qin, B-D. Wang, Z-Y. Yang, K-C. Yu, A ratiometric fluorescent chemosensor for Zn^{2+} in aqueous solution through an ESIPT coupled AIE process, Sensors Actuators B. 224 (2016) 892-898. https://doi.org/10.1016/j.snb.2015.10.110.

[30] J. Li, T. Liu, F. Huo, J. Chao, Y. Zhang, C. Yin, UV and fluorescent spectra study the reaction between 1, 8-Naphthalimide derivative and hypochlorite their applications, Spectrochim Acta A Mol Biomol Spectrosc. 174 (2017) 17-24. https://doi.org/10.1016/j.saa.2016.11.019.

[31] H. Zhang, T. Liu, C. Yin, Y. Wen, J. Chao, Y. Zhang, F. Huo, A novel ratiometric fluorescent probe based on 1, 8-naphthalimide for the detection of Ho(3+) and its bioimaging, Spectrochim Acta A Mol Biomol Spectrosc. 174 (2017) 230-235. https://doi.org/10.1016/j.saa.2016.11.039.

[32] H. Zhang, C. Yin, T. Liu, Y. Zhang, F. Huo, "Turn-on" fluorescent probe detection of Ca(2+) ions and applications to bioimaging, Spectrochim Acta A Mol Biomol Spectrosc. 180 (2017) 211-216. https://doi.org/10.1016/j.saa.2017.03.023.

[33] J. Li, P. Li, F-J. Huo, C. Yin, T. Liu, J. Chao, Y. Zhang, Ratiometric fluorescent probes for ClO^- and invivo applications, Dyes Pigments. 130 (2016) 209-215. https://doi.org/10.1016/j.dyepig.2016.02.024.

[34] J. Zhou, L. Li, W. Shi, X. Gao, X. Li, H. Ma, HOCl can appear in the mitochondria of macrophages during bacterial infection as revealed by a sensitive mitochondrial-targeting fluorescent probe, Chem. Sci. 6 (2015) 4884-4888. https://doi.org/10.1039/C5SC01562F.

[35] X. Jin, L. Hao, Y. Hu, M. She, Y. Shi, M. Obst, J. Li, Z. Shi, Two novel fluorescein-based fluorescent probes for hypochlorite and its real applications in tap water and biological imaging, Sensors Actuators B. 186 (2013) 56-60. https://doi.org/10.1016/j.snb.2013.05.079.

[36] J. Lv, Y. Chen, F. Wang, T. Wei, Z. Zhang, J. Qiang, X. Chen, A mitochondria-targeted fluorescent probe based on fluorescein derivative for detection of hypochlorite in living cells, Dyes Pigments. 148 (2018) 353-358. https://doi.org/10.1016/j.dyepig.2017.09.037.

[37] X. Chen, X. Wang, S. Wang, W. Shi, K. Wang, H. Ma, A Highly Selective and Sensitive Fluorescence Probe for the Hypochlorite Anion, Chem. - Eur. J. 14(2008):4719-4724. https://doi.org/10.1002/chem.200701677.

[38] W-Y. Lin, L-L Long, B-B Chen, W. Tan, A Ratiometric Fluorescent Probe for Hypochlorite Based on a Deoximation Reaction, Chem. - Eur. J. 15 (2009) 2305-2309. https://doi.org/10.1002/chem.200802054.

[39] A. Signore, S.J. Mather, G. Piaggio, G. Malviya, R.A. Dierckx, Molecular Imaging of Inflammation/Infection: Nuclear Medicine and Optical Imaging Agents and Methods, Chem. Rev. 110 (2010) 3112-3145. https://doi.org/10.1021/cr900351r.

[40] R. Zhang, B. Song, Z. Dai, Z. Ye, Y. Xiao, Y. Liu, J. Yuan, Highly sensitive and selective phosphorescent chemosensors for hypochlorous acid based on ruthenium(II) complexes, Biosens. Bioelectron. 50 (2013) 1-7.

https://doi.org/10.1016/j.bios.2013.06.005.

[41] B. Tang, F. Yu, P. Li, L. Tong, X. Duan, T. Xie, X. Wang, A Near-Infrared Neutral pH Fluorescent Probe for Monitoring Minor pH Changes: Imaging in Living HepG2 and HL-7702 Cells, J. Am. Chem. Soc. 131 (2014) 3016-3023. https://doi.org/10.1021/ja809149g.

[42] Z. Yang, M. Wang, M. She, B. Yin, Y. Huang, P. Liu, J. Li, S. Zhang, New aliphatic and aromatic dialdehyde bridged turn-on probes for hypochlorite detection in biological samples based on bis(fluorescein), Sensors Actuators B. 202 (2014) 656-662. https://doi.org/10.1016/j.snb.2014.05.130.

[43] S-Y. Yu, C-Y. Hsu, W-C. Chen, L-F. Wei, S-P .Wu, A hypochlorous acid turn-on fluorescent probe based on HOCl-promoted oxime oxidation and its application in cell imaging, Sensors Actuators B. 196 (2014) 203-207. https://doi.org/10.1016/j.snb.2014.01.121.

[44] M. Cao, H. Chen, D. Chen, Z. Xu, S.H. Liu, X. Chen, J. Yin, Naphthalimide-based fluorescent probe for selectively and specifically detecting glutathione in the lysosomes of living cells, Chem. Commun. 52 (2015) 721-724. https://doi.org/10.1039/c5cc08328a.

[45] P. Ma, B. Zhang, Q. Diao, L. Li, Y. Sun, X. Wang, D. Song, A water-soluble fluorescent probe for ClO^- and Cd^{2+} under physiological pH and its applications in living cells imaging, Sensors Actuators B. 233 (2016) 639-645. https://doi.org/10.1016/j.snb.2016.04.142.

[46] S-L. Wang, L. Zhong, Q-H. Song, Sensitive and Selective Detection of Phosgene, Diphosgene, and Triphosgene by a 3,4- Diaminonaphthalimide in Solutions and the Gas Phase, Chem. - Eur. J. 24 (2018) 1-8 https://doi.org/10.1002/chem.201800051.

[47] B. Zhu, L. Wu, Y. Wang, M. Zhang, Z. Zhao, C. Liu, Z. Wang, Q. Duan, P. Jia, A highly selective and ultrasensitive ratiometric far-red fluorescent probe for imaging endogenous peroxynitrite in living cells, Sensors Actuators B. 259 (2018) 797-802. https://doi.org/10.1016/j.snb.2017.12.135.

[48] Y. Yang, C. Yin, F. Huo, J. Chao, Y. Zhang, S. Jin, Simple 1,8-diaminonaphthalene-based fluorescence chemosensor for hypochlorites and its practical application, Sensors Actuators B. 199 (2014) 226-231. https://doi.org/10.1016/j.snb.2014.03.105.

[49] H. Xiao, K. Xin, H. Dou, G. Yin, Y. Quan, R. Wang, A fast-responsive mitochondria-targeted fluorescent probe detecting endogenous hypochlorite in living RAW 264.7 cells and nude mouse, Chem. Commun. 51 (2015) 1442-1445. https://doi.org/10.1039/c4cc07411d.

[50] J. Li, C. Yin, T. Liu, Y. Wen, F. Huo, A new mechanism-based fluorescent probe for the detection of ClO^- by

UV–vis and fluorescent spectra and its applications, Sensors Actuators B. 252 (2017) 1112-1117. https://doi.org/10.1016/j.snb.2017.07.171.

[51] M-M Yu, W-W. Du, H. Li, H-Y. Zhang, Z-X. Li, Near-infrared ratiometric fluorescent detection of arginine in lysosome with a new hemicyanine derivative, Biosens. Bioelectron. 92 (2017) 385-389. https://doi.org/10.1016/j.bios.2016.10.090.

[52] Z-X Li, W-Y. Zhang, C-X. Liu, M-M. Yu, H-Y. Zhang, L. Guo, L-H. Wei, A colorimetric and ratiometric fluorescent probe for hydrazine and its application in living cells with low dark toxicity, Sensors Actuators B. 241 (2017) 665-671. https://doi.org/10.1016/j.snb.2016.10.141.

[53] L. Zang, C. Liang, Y. Wang, W. Bu, H. Sun, S. Jiang, A highly specific pyrene-based fluorescent probe for hypochlorite and its application in cell imaging, Sensors Actuators B. 211 (2015) 164-169. https://doi.org/10.1016/j.snb.2015.01.046.

[54] H. Zhu, J. Fan, J. Wang, H. Mu, X. Peng, An "enhanced PET"-based fluorescent probe with ultrasensitivity for imaging basal and elesclomol-induced HClO in cancer cells, J. Am. Chem. Soc. 136 (2014) 12820-12823. https://doi.org/10.1021/ja505988g.

[55] J. Zha, B. Fu, C. Qin, L. Zeng, X. Hu, A Ratiometric Fluorescent Probe for Rapid and Sensitive Visualizing Hypochlorite in Living Cells, Rsc Adv. 4 (2014) 59535-59540. https://doi.org/10.1039/c4ra10633d.

[56] Y-R. Zhang, Y. Liu, X. Feng, B-X. Zhao, Recent progress in the development of fluorescent probes for the detection of hypochlorous acid, Sensors Actuators B. 240 (2017) 18-36. https://doi.org/10.1016/j.snb.2016.08.066.

[57] M. Rosenberg, K.R. Rostgaard, Z. Liao, A.Ø. Madsen, K.L. Martinez, T. Vosch, B.W. Laursen, Design, synthesis, and time-gated cell imaging of carbon-bridged triangulenium dyes with long fluorescence lifetime and red emission, Chem. Sci. 9 (2018) 3122-3130. https://doi.org/10.1039/C8SC00089A.

[58] P. Xing, Y. Feng, Y. Niu, Q. Li, Z. Zhang, L. Dong, C. Wang, A water- soluble, two- photon probe for imaging endogenous hypochlorous acid in live tissue, Chem - Eur. J. 24 (2018) 1-7. https://doi.org/10.1002/chem.201800249.

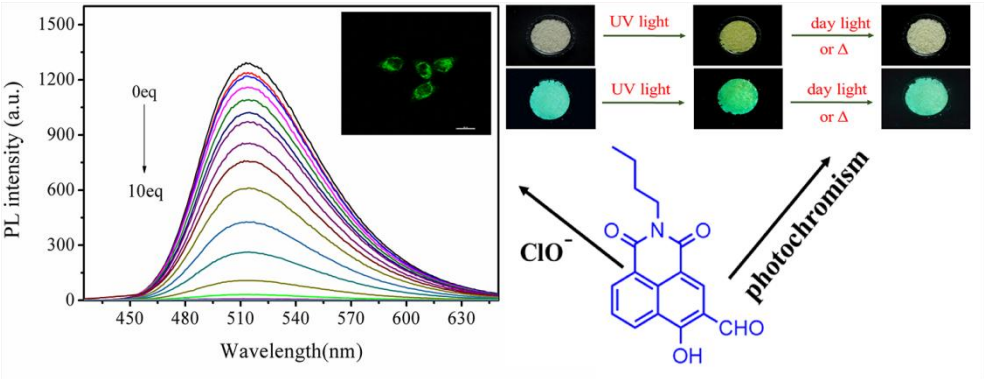

Graphical abstract

Highlights

- This is an interesting naphthalimide-based bifunctional material with reversible photochromic behavior and ClO^- recognition effect.
- The compound **BHC** exhibits a rare naphthalimide-based ESIPT mechanism for photochromic properties and fatigue resistance.
- This is a completely water soluble fluorescent probe
- The probe **BHC** is capable of simultaneously detecting ClO^- in aqueous solution and living cells with high sensitivity and selectivity, and exhibits obvious "on-off" fluorescence.
- Probe **BHC** exhibited ideal properties including high sensitive, good selectivity and short response time.